JOURNAL OF NANO- AND ELECTRONIC PHYSICS
Vol. **11** No 3, 03021(5pp) (2019)

ЖУРНАЛ НАНО- ТА ЕЛЕКТРОННОЇ ФІЗИКИ
Том **11** № 3, 03021(5cc) (2019)

Sol-Gel Synthesis, Structure and Optical Properties of Nickel-Manganese Ferrites

V.S. Bushkova[1,*], I.P. Yaremiy[1], B.K. Ostafiychuk[1,2], N.I. Riznychuk[1], R.S. Solovei[1]

[1] *Vasyl Stefanyk Precarpathian National University, 57 Shevchenko St., 76025 Ivano-Frankivsk, Ukraine*
[2] *Institute of Metal Physics, National Academy of Science, 36 Acad. Vernadsky Boulevard, 03680 Kyiv, Ukraine*

(Received 25 October 2018; revised manuscript received 12 June 2019; published online 25 June 2019)

The nickel ferrite $NiFe_2O_4$ obtained by ceramic technology has been widely studied due to its tremendous properties like high electromagnetic performance, excellent chemical stability and mechanical hardness, and moderate saturation magnetization, making it a good contender for the application as soft magnets and low loss materials at high frequencies. The structure, mechanical, magnetic, electrical and dielectric properties of nickel ferrite are dependent upon several factors including the method of preparation, sintering time and temperature, chemical composition, type and amount of dopant, grain structure. The sol-gel with participation of auto-combustion (SGA) technique was used for the synthesis of $Ni_{1-x}Mn_xFe_2O_4$ (x = 0.0, 0.1, 0.2, 0.3, 0.4, 0.5 and 0.6) nanoparticle ferrites. The mixed solution was dried at a temperature around 403 K. During evaporation the solution became viscous and finally formed a xerogel. At further temperature rise, the organic constituents are decomposed with the generation of gases such as CO_2, N_2 and H_2O; therefore the xerogel automatically ignited. The auto-combustion was completed within a few seconds, yielding the nanopowders of ferrites. Structural parameters, morphology and optical properties were investigated. The XRD results confirm single-phase formation of the as-prepared samples with $0.0 \le x \le 0.4$ having the Fd3m space group. The $Ni_{0.5}Mn_{0.5}Fe_2O_4$ and $Ni_{0.4}Mn_{0.6}Fe_2O_4$ powders except the spinel phase contain also additional FeO and Ni phases. The crystallite sizes (27-43 nm) decrease and the lattice parameters (0.8343-0.8459 nm) increase, while the Mn concentration increases. Morphological observations reveal that the crystallinity decreases significantly with increasing Mn content meanwhile the particle size becomes more uniform. It was found that the optical band gap increases with increasing concentration of Mn^{2+} ions in the ferrite structure. The band gap is in the range from 2.00 eV to 3.26 eV.

Keywords: Ferrite, Nanopowder, Sol-gel auto-combustion, Band gap energy.

DOI: 10.21272/jnep.11(3).03021 PACS numbers: 82.45.Yz, 82.47.Uv, 71.20.Tx

1. INTRODUCTION

The ferrites have various technological applications, which include spintronic devices, magnetic refrigeration, high-density recording devices, magneticfluids, and magnetic coating [1-3]. The $Ni_{1-x}Mn_xFe_2O_4$ ferrites are ceramic ferromagnetic materials, which possess excellent magnetic and electrical properties useful for electromagnetic applications [4]. The nanoparticles of ferrite materials play a special role. If they are not currently in use, they are already at the implementation stage in the energy sector (for example, to increase the efficiency of conversion of light energy in solar cells), in biology (the basis for plasmon analyzers of biological microobjects), in agrarian sector (increase of resistance against virus diseases of rhizomes) and in medicine (targeted drug delivery) [5].

Among the various spinel ferrites, the $NiFe_2O_4$ has been used as a potential catalyst in opto-magnetic and electronic devices and photo-catalysts [6]. Mainly, the cation distributions in sub-lattices of spinel influence the magnetic properties of ferrites. The nickel ferrite is an inverse spinel, in which half of the ferric ions preferentially fill the tetrahedral sites (A), and the other ions occupy the octahedral sites (B). The Ni^{2+} ions preferentially occupy B-sites [7]. It is known [8], that in manganese-doped ferrites, the Mn ions do not have strong site preference to A or B-sites. The structure and magnetic properties of ferrites are known to be very sensitive to preparation methods [9], the sintering process and additive substitutions [10]. In addition, surface spins and reduction of particle sizes also play an important role in the magnetic parameters of ferrite nanoparticles. Therefore, to achieve materials of the desired physical and chemical properties, the preparation of ferrite nanoparticles through different routes has become an essential part of research and its development.

Therefore, keeping in view the high demand and importance of magnetic ferrite nanoparticles, the aim of the present paper is to study the role of Mn^{2+} ions substitution on structure, optical and magnetic properties of $NiFe_2O_4$ prepared by the SGA technology.

2. EXPERIMENTS

The substituted by manganese ions nickel ferrites with the formula $Ni_{1-x}Mn_xFe_2O_4$ (x = 0.0, 0.1, 0.2, 0.3, 0.4, 0.5 and 0.6) were prepared by SGA technique. At room temperature, the X-ray diffraction patterns on Dron 7 X-ray diffractometer were recorded using CuKα radiation. The data processing of the diffractometric experiment was carried out using FullProf program. The scanning electronic microscopy (SEM) of nickel-manganese ferrite powders was performed with a Hitachi S-4700 electron microscope operating at 20.0 kV. Light absorption properties of $Ni_{1-x}Mn_xFe_2O_4$ nanocrystals were studied by a UV-Vis spectrophotometer (ULAB 102 UV model).

* bushkovavira@gmail.com

3. RESULTS AND DISCUSSION

3.1 X-ray Diffraction (XRD)

Fig. 1 shows the X-ray diffraction patterns of nickel-manganese ferrite powders. The XRD analysis of samples $Ni_{0.9}Mn_{0.1}Fe_2O_4$, $Ni_{0.8}Mn_{0.2}Fe_2O_4$, $Ni_{0.7}Mn_{0.3}Fe_2O_4$ and $Ni_{0.6}Mn_{0.4}Fe_2O_4$ revealed the formation of only ferrite phase. The peaks are indexed to (111), (220), (311), (222), (400), (422), (511) and (440) planes, which correspond to the cubic structure of spinel space group Fd3m.

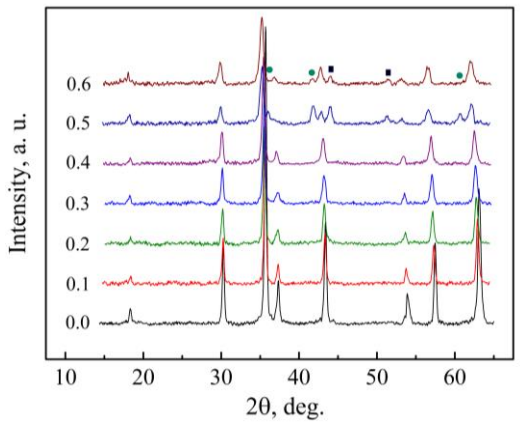

Fig. 1 – X-ray spectra of Ni1-xMnxFe2O4 powders, where ■ is the Ni phase and ● – FeO

The $Ni_{0.5}Mn_{0.5}Fe_2O_4$ and $Ni_{0.4}Mn_{0.6}Fe_2O_4$ powders except the spinel phase contain also additional phases. For example, for $Ni_{0.5}Mn_{0.5}Fe_2O_4$ sample, peaks 35.96 °, 41.78 °, 60.61 ° at angles 2θ are observed that corresponds to the content of FeO phase and peaks 44.01 °, 51.23 ° – to the Ni phase. Similarly, for $Ni_{0.4}Mn_{0.6}Fe_2O_4$ ferrite, the peaks 35.90 °, 41.70 °, 60.59 ° from FeO and 44.01 °, 51.30 ° from Ni are fixed. The $Ni_{0.5}Mn_{0.5}Fe_2O_4$ ferrite contains 15 % FeO and 15 % Ni, and the $Ni_{0.4}Mn_{0.6}Fe_2O_4$ sample contains less number of additional phases – 3 % FeO and 6 % Ni. Additional phases of these samples can be eliminated by further sintering at 500 °C for 2 h.

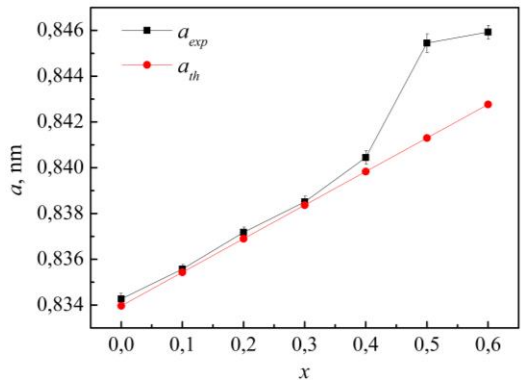

Fig. 2 – Lattice parameters of $Ni_{1-x}Mn_xFe_2O_4$ powders

The average size of coherent scattering regions (CSR) in the powders of nickel-manganese ferrites was found from the peak (311) using the Scherrer equation:

$$\langle D\rangle = \frac{0.9\lambda}{\beta\cdot\cos\theta}, \qquad (1)$$

where β is the effective half-width of the diffraction peak for X-rays with wavelength λ at an angle 2θ. The average size of CSRs of powders was in the range of 27-43 nm.

Lattice constant of $Ni_{1-x}Mn_xFe_2O_4$ was determined from X-ray data analysis. The values of the lattice parameter increase with an increase in manganese content from 0.8343 nm to 0.8459 nm (Fig. 2). The results are in good agreement with Xu et al. [8]. With increasing Mn-concentration, the lattice parameters of Ni-Mn ferrites increase. It is due to the replacement of the smaller ionic radius of Ni^{2+} by bigger ionic radius of Mn^{2+}, because tetrahedral and octahedral ionic radii of Ni^{2+} and Mn^{2+} are 0.055 nm, 0.069 nm and 0.066 nm, 0.080 nm, respectively. [11]. In Table 1, the calculated crystallite sizes D, lattice parameters a, X-ray density d_x, and molar mass for the $Ni_{1-x}Mn_xFe_2O_4$ powders are given. The calculated X-ray density is in the range of 5.09-5.36 g/cm^3.

Table 1 – Structural parameters calculated from the XRD patterns of the $Ni_{1-x}Mn_xFe_2O_4$

x	D, nm	a, nm	M, g·mol^{-1}	d_x, g·cm^{-3}
0.0	43	0.8343	234.4	5.36
0.1	41	0.8356	234.0	5.33
0.2	38	0.8372	233.6	5.29
0.3	37	0.8385	233.3	5.25
0.4	35	0.8405	232.9	5.21
0.5	30	0.8455	232.5	5.11
0.6	27	0.8459	232.1	5.09

The theoretical lattice constant a_{th} for nickel-manganese ferrite powders can be calculated by the relation:

$$a_{th} = \frac{8}{3\sqrt{3}}\left[\left(r_A + r_0\right) + \sqrt{3}\left(r_B + r_0\right)\right], \qquad (2)$$

where r_0 is the radius of oxygen ion (0.132 nm), r_A and r_B are the ionic radii of tetrahedral and octahedral sites, respectively.

According to the Ref. [11], the theoretical ion radii r_A and r_B are calculated using the following relations:

$$r_A = r\left(Fe^{3+}\right), \qquad (3)$$

$$r_B = \frac{1}{2}\left[\left(1-x\right)\cdot r\left(Ni^{2+}\right) + x\cdot r\left(Mn^{2+}\right) + r\left(Fe^{3+}\right)\right], \qquad (4)$$

where $r(Ni^{2+})$, $r(Mn^{2+})$, $r(Fe^{3+})$ are the radii of the corresponding ions depending on the coordination number.

It is known that in the structure of a spinel, the coordinate number is $k = 4$ for two valence metal ions and 6 – for three valence. For Goldschmidt, the radii $r(Ni^{2+}) = 0.069$ nm, $r(Mn^{2+}) = 0.080$ nm and $r(Fe^{3+}) = 0.0645$ nm. The dependence of the theoretical and experimental values of the lattice parameter is illustrated in Fig. 3, which shows that the lattice parameter increases with increasing Mn^{2+} content in the $Ni_{1-x}Mn_xFe_2O_4$ system. Thus, the theoretical and experimental values of lattice parameters for $x \le 4$ are consistent with each other. For $x \ge 5$, a deviation of the lattice parameter a_{exp} from a_{th} is observed. The devia-

tion is due to additional phases of FeO and Ni, which are associated with the features of the SGA synthesis. In this connection, the number of Mn^{2+} cations with a large ion radius in the spinel structure is much larger than the number of Ni^{2+} and Fe^{3+} cations.

From Fig. 3, it is observed that ionic radius r_A on A-site does not depend on the concentration of Mn^{2+} ions, and ionic radius r_B on B-site increases with increasing Mn^{2+} content. This is due to the fact that Ni^{2+} ions with smaller ionic radius are replaced by Mn^{2+} ions with larger ionic radius in B-site.

For the case of an ideal spinel, the oxygen parameter u, which characterizes the location of oxygen ions in the crystalline lattice, is 0.375. However, in real ferrites, the crystal lattice is slightly deformed due to the action of various factors, such as the size of substitution ions and the force of interaction between them. For example, in zinc and iron ferrites, $u > 0.375$ because oxygen ions are shifted from the ideal location in the direction (111), which leads to the increase of the distance between the A-sites, and distance between the B-sites is reduced. Consequently, the oxygen parameter depends on the chemical composition of the ferrites, as well as on the method of their receipt.

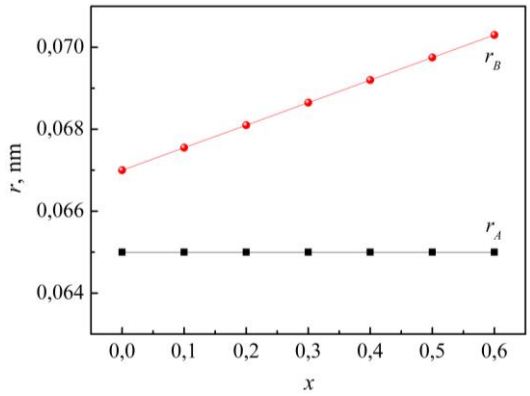

Fig. 3 – The mean ionic radii per molecule of the A and B-sites

The anion parameter for the $Ni_{1-x}Mn_xFe_2O_4$ system is determined by the ratio [12]:

$$u = \frac{1}{\sqrt{3}a} \cdot \left(r_A + r_0\right) + \frac{1}{4}. \qquad (5)$$

It is known that the elementary cell is divided into eight octants. The location of ions is the same in the neighboring octants, which are separated by edge and is different in the octants that are separated by a face. The radius of the sphere inscribed in the tetrahedron of undistorted oxygen sub-lattice is 0.227 of the radius of the oxygen ion O^{2-}. The radius of the sphere inscribed in the octahedron is a slightly larger – $r_B = 0.418 \cdot r_0$. The oxygen parameter u decreases (0.3863-0.3850) while the Mn-concentration increases.

3.2 Morphology Study

The SEM micrographs of prepared $Ni_{1-x}Mn_xFe_2O_4$ particles are given in Fig. 4a, b. Fig. 4a shows the surface of the pure nanocrystalline $NiFe_2O_4$ sample, which appears as accumulative globular particles. The average diameter of these particles is about 50 nm, which is in agreement with average size of CSRs calculated by the Scherrer equation. The morphological features of $Ni_{0.4}Mn_{0.6}Fe_2O_4$ powder is illustrated in Fig. 4b. The presence of porous agglomerates composed of individual spherical particles is shown in Fig. 4b. The average size of agglomerates does not exceed 150 nm.

3.3 Optical Studies

In Fig. 5, the UV-V is absorption spectra of the $Ni_{1-x}Mn_xFe_2O_4$ ferrite powders are shown. Using the fundamental relationships [13], the absorption coefficient α of the particles was calculated.

Using the Tauc's relation, the band gap of Ni-Mn ferrites is determined as [14]:

$$\alpha h\nu = A\left(h\nu - E_g\right)^n, \qquad (6)$$

where E_g and $h\nu$ are the band gap and the photon energy in eV. For all samples, the graph of $(\alpha h\nu)^2$ versus $h\nu$ was plotted (Fig. 6) to determine the energy band gap.

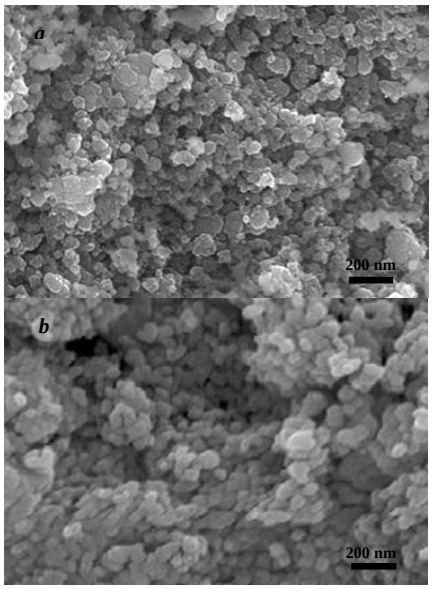

Fig. 4 – SEM micrograph of Ni-Mn ferrites: a – $NiFe_2O_4$ and b – $Ni_{0.4}Mn_{0.6}Fe_2O_4$

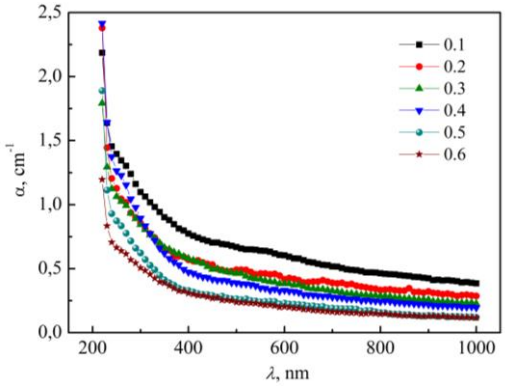

Fig. 5 – The optical absorption spectra of Ni.Mn ferrites

The value of the energy band gap was obtained by extrapolation of the line at $\alpha = 0$.

The energy band gap of SGA-powder nickel ferrite with an average particle size of 43 nm is equal to 2.00 eV [7]. On the other hand, $E_g = 1.91$ eV for $NiFe_2O_4$ with a particle size of 61 nm. For all other samples, the values of the energy band gap are listed in Table 2 and were found in the range of 2.00-3.26 eV. There is blue shift for all Mn-doped samples indicating that these nanoparticles may have visible-light photoactivity. This is mainly attributed to the reduction in crystallite size of powders as Mn content increases.

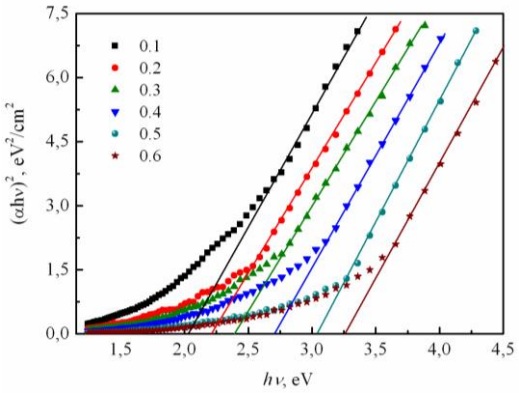

Fig. 6 – Tauc plot of $(\alpha h\nu)^2$ as a function of photon energy $h\nu$

Table 2 – Optical characteristics of Ni-Mn ferrites

x	λ, nm	E_g, eV	E_g [6], eV
0.0	620	2.00	2.02
0.1	612	2.03	2.11
0.2	562	2.21	2.17
0.3	520	2.39	2.25
0.4	459	2.71	2.33
0.5	409	3.04	2.42
0.6	381	3.26	–

In Ref. [6], $Ni_{1-x}Mn_xFe_2O_4$ particles prepared by a facile microwave combustion method using urea as the fuel were studied by UV-Vis spectroscopy. The average crystallite sizes of the powders were in the range from 11.49 nm to 17.24 nm, moreover, the particle size decreases with increase of Mn^{2+} ions. The values of band gap were found in the range of 2.02-2.42 eV. The increase in band gap and decrease in refractive index have been observed also with increasing concentration of Mn^{2+} ions. Thus, the band gap of Ni-Mn ferrite powders increases with manganese concentration due to the decrease in average crystallite sizes. The decreasing crystallite size of Ni-Mn ferrite powders leads to the shift in E_g that is the result of quantum confinement effects. Therefore, these samples can be used for making optical devices.

4. CONCLUSIONS

The $Ni_{1-x}Mn_xFe_2O_4$ ferrites were synthesized by the SGA technology. For samples with $0.0 \le x \le 0.4$, single-phase powders with a cubic structure of spinel space group Fd3m were obtained. Other samples were non-phase and contain additional FeO and Ni phases. The size of powders was found to be in the range from 27 to 43 nm. The lattice parameter increases from 0.8343 nm to 0.8459 nm because the replacement of smaller ionic crystal radius of Ni^{2+} by larger Mn^{2+} occurs. The major effect on the surface morphology of the Ni-Mn ferrites had additional manganese. The addition of Mn^{2+} ions contributes to the more uniform particle size and causes its decrease. X-ray density decreases with increasing Mn concentration in the Ni-Mn ferrites and is in the range of 5.09-5.36 g/cm^3.

For all investigated powders, it was revealed that the allowed direct transition of electrons from the valence band to the conduction band is inherent. The increase of Mn^{2+} cations in the Ni-Mn ferrites leads to an increase of the optical band gap from 2.00 eV to 3.29 eV.

REFERENCES

1. D.T.T. Nguyet, N.P. Duong, L.T. Hung, T.D. Hien, T. Satoh, *J. Alloys Compd.* **509**, 6621 (2011).
2. B.K. Ostafiychuk, V.S. Bushkova, V.V. Moklyak, R.V. Ilnitsky, *Ukr. J. Phys.* **60**, 1234 (2015).
3. Abdullah Ceylan, Sadan Ozcan, C. Ni, S. Ismat Shah, *J. Magn. Magn. Mater.* **320**, 857 (2008).
4. J. Hu, T.W. Odom, C.M. Lieber, *Acc. Chem. Res.* **32**, 435 (1999).
5. S.D. Bader, *Rev. Modern Phys.* **78**, 1 (2006).
6. C. Barathiraja, A. Manikandan, A.M. Uduman Mohideen, S. Jayasree, S. Arul Antony, *J. Supercond. Nov. Magn.* (2015).
7. Vira S. Bushkova, Ivan P. Yaremiy, *J. Magn. Magn. Mater.* **461**, 37 (2018).
8. J. Xu, L. Ma, Z.Z. Li, L. L. Lang, W.H. Qi, G.D. Tang, L.Q. Wu, L.C. Xue, G.H. Wu, *phys. status solidi b* **252** 2820 (2015).
9. V.S. Bushkova, B.K. Ostafiychuk, *Powder Metall. Metal Ceram.* **54**, 509 (2016).
10. V.S. Bushkova, *J. Nano- Electr. Phys.* **8**, 01002 (2016).
11. Hafiz M.I. Abdallah, Thomas Moyo, *J. Magn. Magn. Mater.* **361**, 170 (2014).
12. M.A. Ahmed, E. Ateia, L.M. Salah, A.A. El-Gamal, *Mater. Chem. Phys.* **92**, 310 (2005).
13. M. Srivastava, A.K. Ojha, S. Chaubey, and A. Materny, *J. Alloy. Compd.* **481**, 515 (2009).
14. D. Rekha, R. Subasri, K. Radha, H. Pramod Borse, *Solid State Commun.* **151**, 470 (2011).

Золь-гель синтез, структура та оптичні властивості нікель-марганцевих феритів

В.С. Бушкова[1], І.П. Яремій[1], Б.К. Остафійчук[1,2], Н.І. Різничук[1], Р.С. Соловей[1]

[1] *Прикарпатський національний університет ім. В. Стефаника, 57, вул. Шевченка, 76025 Івано-Франківськ, Україна*

[2] *Інститут металофізики ім. Г.В. Курдюмова, НАНУ, 36, бульвар Акад. Вернадського, 03680 Київ, Україна*

Властивості фериту нікелю $NiFe_2O_4$, отриманого за керамічною технологією, є широко вивчені, оскільки він володіє високою електромагнітною продуктивністю, відмінною хімічною стабільністю і механічною твердістю, а також помірною намагніченістю насичення, що робить його хорошим претендентом у застосуванні як м'якого магнітного матеріалу з низькими втратами на високих частотах. Структура, механічні, магнітні, електричні та діелектричні властивості фериту нікелю залежать від декількох факторів, включаючи спосіб приготування, час і температуру спікання, хімічний склад, тип і кількість легуючої домішки та зернову структуру. Для синтезу $Ni_{1-x}Mn_xFe_2O_4$ (x = 0.0; 0.1; 0.2; 0.3; 0.4; 0.5 і 0.6) наночастинок феритів був використаний метод золь-гель за участі автогоріння (ЗГА). Отриманий розчин було висушено за температури близько 403 К. Під час випарювання розчин поступово ставав в'язкими, в результаті чого сформувався ксерогель. За подальшого підвищення температури органічні складові розклалися з утворенням таких газів, як CO_2, N_2 і H_2O. Процес автоматичного згорання ксерогелю завершився протягом декількох секунд, що призвело до утворення нанопорошків феритів. Досліджено структурні параметри, морфологію та оптичні властивості порошків. Результати Х-променевих досліджень підтверджують утворення однофазових порошків для $0.0 \le x \le 0.4$ просторової групи Fd3m. Порошки $Ni_{0.5}Mn_{0.5}Fe_2O_4$ та $Ni_{0.4}Mn_{0.6}Fe_2O_4$, крім фази шпінелі, містять також додаткові фази FeO та Ni. Розміри кристалітів (27-43 нм) зменшуються, а параметр ґратки (0.8343-0.8459 нм) збільшується при збільшенні концентрації іонів Mn. Морфологічні спостереження показують, що кристалічність істотно зменшується при збільшенні вмісту Mn, а розмір частинок стає більш однорідним. Встановлено, що оптична ширина забороненої зони збільшується з ростом концентрації іонів Mn^{2+} у феритовій структурі. Ширина забороненої зони знаходиться в діапазоні від 2.00 еВ до 3.26 еВ.

Ключові слова: Ферит, Нанопорошок, Золь-гель за участі автогоріння, Ширина забороненої зони.